

LA-UR-14-24435

Approved for public release; distribution is unlimited.

Title: SEM in situ MiniCantilever Beam Bending of U-10Mo/Zr/Al Fuel Elements

Author(s): Mook, William
Baldwin, Jon K.
Martinez, Ricardo M.
Mara, Nathan A.

Intended for: Report

Issued: 2014-06-16

Disclaimer:

Los Alamos National Laboratory, an affirmative action/equal opportunity employer, is operated by the Los Alamos National Security, LLC for the National Nuclear Security Administration of the U.S. Department of Energy under contract DE-AC52-06NA25396. By approving this article, the publisher recognizes that the U.S. Government retains nonexclusive, royalty-free license to publish or reproduce the published form of this contribution, or to allow others to do so, for U.S. Government purposes. Los Alamos National Laboratory requests that the publisher identify this article as work performed under the auspices of the U.S. Department of Energy. Los Alamos National Laboratory strongly supports academic freedom and a researcher's right to publish; as an institution, however, the Laboratory does not endorse the viewpoint of a publication or guarantee its technical correctness.

SEM *in situ* MiniCantilever Beam Bending of U-10Mo/Zr/Al Fuel Elements
Authors: W.M. Mook, J.K. Baldwin, R. Martinez, N.A. Mara

Center for Integrated Nanotechnologies (MPA-CINT)
Los Alamos National Laboratory
Los Alamos, NM 87545, USA

April 21, 2014

Abstract

In this work, the fracture behavior of Al/Zr and Zr/dU-10Mo interfaces was measured via the minicantilever bend technique. The energy dissipation rates were found to be approximately 3.7-5 mJ/mm² and 5.9 mJ/mm² for each interface, respectively. It was found that in order to test the Zr/U-10Mo interface, location of the hinge of the cantilever was a key parameter. While this test could be adapted to hot cell use through careful alignment fixturing and measurement of crack lengths with an optical microscope (as opposed to SEM, which was used here out of convenience), machining of the cantilevers via MiniMill in such a way as to locate the interfaces at the cantilever hinge, as well as proper placement of a femtosecond laser notch will continue to be key challenges in a hot cell environment.

Introduction:

Recent research into dU-10Mo/Zr/Al plate fuel assemblies has illustrated the importance of fundamentally understanding their interfacial mechanical behavior. The parameters and phenomena that have been noted include existence of stress gradients at interfaces and their influence on bond strength [1], and strength and fracture behavior of the various interfaces before and after irradiation [2]. Bend testing [3] and pull testing [4] have been used to gain some insight on the mechanical behavior of the composite plate, but as noted in [5], neither method can isolate the mechanical behavior of a specific bond.

The plate geometry specifications [6, 7], include a dU-10Mo layer 380 microns thick, a Zr interlayer that is 30 microns thick and Al cladding that is 250 microns thick, giving an overall sample thickness of less than 1mm. As a result, conventional macroscopic mechanical tests have had difficulty in gaining insight about the mechanical behavior of individual interfaces. In order to give local information about the deformability of the regions in the vicinity of the interface, in this

work, micromechanical testing utilizing *in-situ* deformation in the SEM of small (sub-millimeter) cantilevers was carried out on surrogate HIPed Al/Al, Al/Zr and Zr/dU-10Mo bonds that were processed using HIP parameters typically used for complete dU-10Mo/Zr/Al plate fuel assemblies [8].

Overview of experiment and analysis

The goal of this work is to develop an experimental method to quantify the adhesion energy (i.e., the toughness) of individual interfaces within a fuel plate assembly. The method should also be executable within a hot cell. The main experimental challenge arises from the geometry of the fuel plate assembly since the interfaces of interest are composed from materials that are sub-mm in thickness. Therefore micromechanical testing inside of a microscope (in this case, a scanning electron microscope) is ideal. In order to drive fracture at this length scale along a specific interface, a notched cantilever beam geometry is used as seen in the schematic in Figure 1. The cantilever beam is bent with a microindenter that tracks both load and displacement while taking images with the microscope. The notch acts as a stress concentrator and a sharp crack should nucleate from it along the interface of interest.

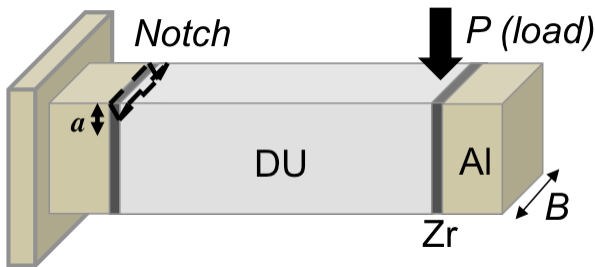


Figure 1: Beam schematic where the Al and DU are 380 μm wide, and the Zr is 30 μm wide. B is the width of the beam and a initially represents the length of the notch, then during testing it is the length of the notch plus crack. Load (P) is applied by the microindenter in order to drive the crack along the prescribed interface.

Ideally for analysis, the structure would deform elastically except for the growing crack. If this were the case, linear elastic fracture mechanics (LEFM) concepts such as fracture toughness (K) could be used to quantify the toughness of the interface. If relatively small amounts of plasticity accompanied crack advance, elastic-plastic fracture mechanics (EPFM) concepts such as the J-integral could be used. However, for the beams tested in this work, there was considerable

plasticity in the aluminum phase. Therefore a global strain energy dissipation (D) approach was used to estimate interfacial adhesion energy. This approach does provide qualitative measurements when dealing with the same geometrical dimensions of the cantilever beam. Since fuel plates will become more brittle after irradiation, it is expected that both strain energy dissipation and J-integral approaches will be applicable for interfacial toughness characterization in the post-irradiated state.

Experimental:

Beam dimensions

The dimensions of the cantilever beams are limited in length by the individual layer thicknesses of the fuel assembly and in cross-sectional area by the maximum load that the indentation load cell can generate (for the CINT SEM-indenter the maximum load is approximately 1 N). Al-Al HIP bonded beams were machined to dimensions of 0.75 mm long with a cross-section of 0.25x0.25 mm. The Al/Zr and Zr/dU-10Mo beams were machined to 0.25 mm long with a nominal cross-section of 0.10 mm x 0.10 mm.

Specimen Preparation: Mini-Milling beams

The minicantilever beams were machined with a MiniMill 4 from MiniTech Industries. This equipment has a positioning accuracy of 2.5 μm that allows the machinist to position an interface at the base of the beam. As will be seen, positioning the interface of interest exactly at the base of the beam is very important in order to drive fracture along the desired interface. The minimum feature size that can be repeatedly milled is between 0.05-0.10 mm. A MiniMill 4 has also been set up in the Sigma Facility at LANL in order to machine dU.

The milling parameters for both the Al/Al and Al/Zr beams were the same; spindle speed = 10,000 rpm, lateral feed rate = 1"/min, depth of cut = 0.001"/pass. The tools were 0.064" diameter diamond-coated carbide end mills. These parameters gave a consistent beam cross-section along its entire length.

Milling dU beams with the MiniMill 4 is more difficult than milling non-dU beams. This is because dU wears the milling tool at a substantially higher rate and results in a large taper toward the base of the beam. Therefore a multi-step process was used such that all of the large milling cuts were made first, then the final shaping cuts were made with a new milling tool bit. The

milling parameters listed above for the Al/Al and Al/Zr beams were used for both steps. The difference in the resulting cantilever beam shape can be seen in Figure 2 where in Figure 2(a) only one end mill was used for the entire process compared to Figure 2(b) where one end mill was used to remove the bulk of the material and then a fresh end mill was used for the finish cuts. In both cases, notches were milled with a FIB along the Zr/dU-10Mo interface.

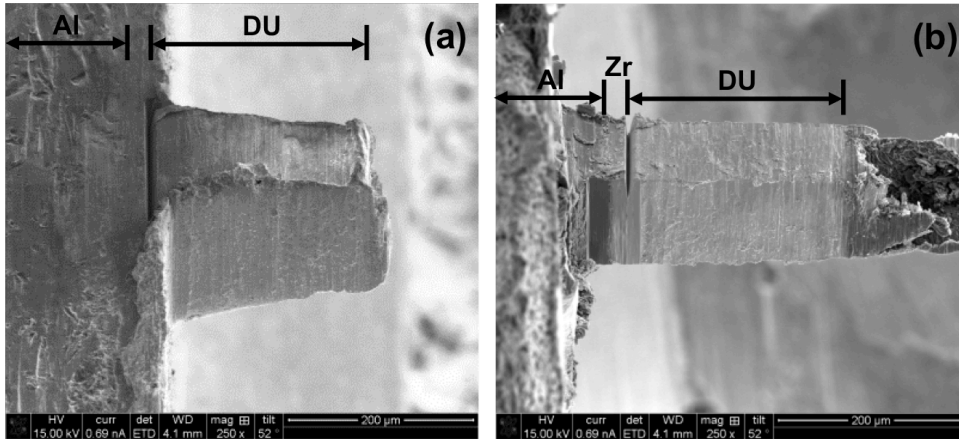


Figure 2: Milling dU-10Mo beams with the MiniMill using the following parameters: spindle speed = 10,000 rpm, lateral feed rate = 1"/min, depth of cut = 0.001"/pass. The tools were 0.064" diamond-coated carbide-end mills where (a) only one end mill was used for the entire process compared to (b) where one end mill was used to remove the bulk of the material and then a fresh end mill was used for the finish cuts. Machining dU quickly blunts the milling tools such that beam taper is inevitable if milling tools are not changed frequently. In both cases, notches were milled with a FIB along the Zr/dU-10Mo interface.

Specimen Preparation: Notch Fabrication

Notches were fabricated by one of two methods; femtosecond laser ablation, or milling with a focused ion beam (FIB). Each method has advantages and disadvantages. The femtosecond laser ablation is fast, taking approximately 1 minute to notch a single beam, although it has lower resolution and spatial accuracy. FIB-milling is relatively slow (it can take 8 hours to notch a single beam) but it is very accurate (spatial accuracy < 100 nm). While the Al-Al and Al-Zr beams could be notched using either method, notching beams with DU required the use of the FIB since the femtosecond laser is located within CINT Gateway at LANL (radioactive materials are not allowed in the CINT Gateway Facility).

Femtosecond laser machining utilized the following parameters and a 20x objective to machine a 10 to 25 μm deep notch at the desired interface: wavelength=776nm, pulse width=800fs, Energy=10mJ, Frequency 4kHz.

FIB milling was carried out on a FEI Helios dual-beam FIB using a Ga ion beam with an accelerating voltage of 30keV and current of 22 nA (both are the maximum values for this instrument which maximizes milling speed). The sample is tilted 52° so that the top of the cantilever beam is perpendicular to the ion beam. The interface that is to be notched is then selected by placing a “regular cross-section” box over it and selecting the milling depth to be approximately 15-20% of the beam thickness. If necessary (and it usually is), the side of the cantilever beam that will be imaged in the SEM during the bend test will need to be smoothed in order to observe the crack growth. This can be accomplished via top-down FIB-milling of the side of the cantilever. A notched and polished cantilever beam can be seen in Figure 2(b).

SEM in-situ beam bending

The cantilever beams were tested inside of one of two SEM's. The FEI Quanta at the Center for Integrated Nanotechnologies (CINT), an international Department of Energy (DOE) user facility at Los Alamos National Laboratory (LANL) was used for non-dU containing materials, while the FEI Helios at the Electron Microscopy Lab (EML) in the Materials Science Laboratory (MSL) at LANL was used for materials that contained dU. The in-house built CINT SEM-Indenter was used to test cantilever beams that could be plastically deformed at loads under 1 N is seen in Figure 3. During testing, the beams were positioned 90° to the SEM electron beam such that the side of the beam and any fracture along the interface in question could be imaged throughout the entire load-unload process. In this way it was possible to monitor interfacial crack length as a function of load in real time. The displacement rate during all of the tests was less than 1 $\mu\text{m}/\text{s}$. The load frame is inherently displacement-controlled, however the displacement rate changes due to compliance of the load cell, i.e., displacement rates during the elastic loading is relatively low while rates during the plastic portion of the bending experiment approach 1 $\mu\text{m}/\text{s}$. Movies of the experiments were created by compiling one image per second from the SEM and syncing to the load-displacement data from the load frame.

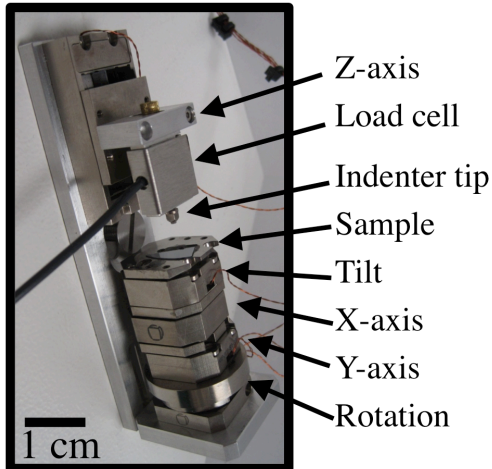


Figure 3: Schematic of custom-built CINT Micromechanical Tester with 1 N load cell used for in-situ straining in the SEM.

For cantilever beams that required higher loads, the Nanoindenter-XP was used (maximum load of 10 N) and conducted at a displacement rate of 50 nm/s. For this test, the bending was intermittently paused and beams were imaged in the SEM when crack growth was evident on the load-displacement curve. The test was then resumed in the nanoindenter.

Results and Discussion:

Al-Al HIP interface:

The Al-Al HIP interface beams were not pre-notched, and their load-displacement response was very repeatable out of three cantilevers tested. A representative load-displacement curve, along with SEM micrographs of the cantilever before and after testing is seen in Figure 4. It is evident that the beam undergoes significant plastic deformation, with no localized fracture near the interface. From these tests, it is clear that a notch or other stress concentrator is necessary to drive crack propagation at the Al-Al interface. This is consistent with prior work on smaller cantilevers [9, 10] which found that in the absence of stress concentrations such as large inclusions or voids at the interface, the Al-Al bond was as strong as the unbonded material.

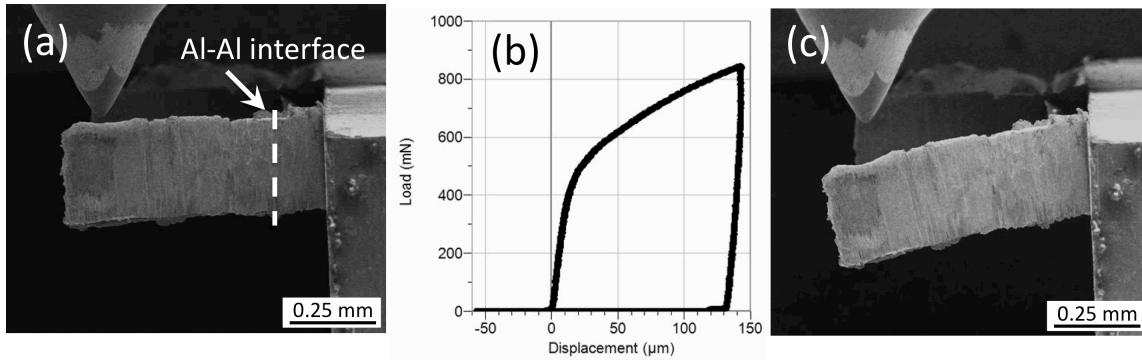


Figure 4: SEM micrographs of the (a) As-milled and (c) deformed Al-Al cantilevers. These samples were not fitted with a pre-notch, and only uniform plastic deformation was observed.

Al/Zr interface:

To assure that fracture propagated along the Al/Zr interface, the samples were notched with a femtosecond laser. The notches made by the laser varied in depth and proximity to the Al/Zr interface, but were in general within 3 μm of the interface and had a depth of approximately 10 μm . Figure 5 shows two deformed Al/Zr cantilevers with notched Al-Zr interfaces. In all tests conducted, fracture occurred at the Al/Zr interface. Interestingly, the position of the notch did not seem to affect the path of the crack, as failure always occurred at the Al/Zr interface, even if the notch was located a few microns from the interface itself. This behavior is evident in the cantilever seen in the foreground of Figure 5, where the notch was located in the Zr, but fracture still proceeded at the Al-Zr interface.

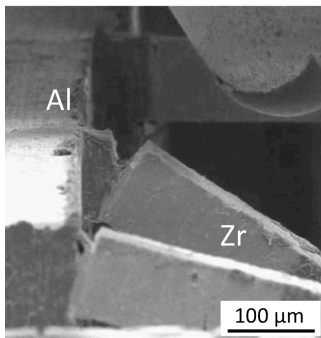


Figure 5: Al/Zr notched beams after bend testing. The notch was made within the Zr layer in the beam in the foreground, however the crack proceeded along the Al/Zr interface.

Figure 6 shows the load-displacement response of the Al/Zr notched beam in addition to images taken from the movie that were used to calculate crack growth. From this data, fracture energy dissipation rates can be calculated [11]. The fracture energy dissipation rate (D) is:

$$D = \frac{dE}{dA} = \frac{1}{2B} \frac{dU}{da};$$

where dE is the total energy dissipated, i.e., it is the area under the load-displacement curve. The new surface area of the crack is dA which is the width of the beam, B , multiplied by twice the new crack length, $2a$, accounting for the two faces of the crack. Calculations can be seen in Table 1.

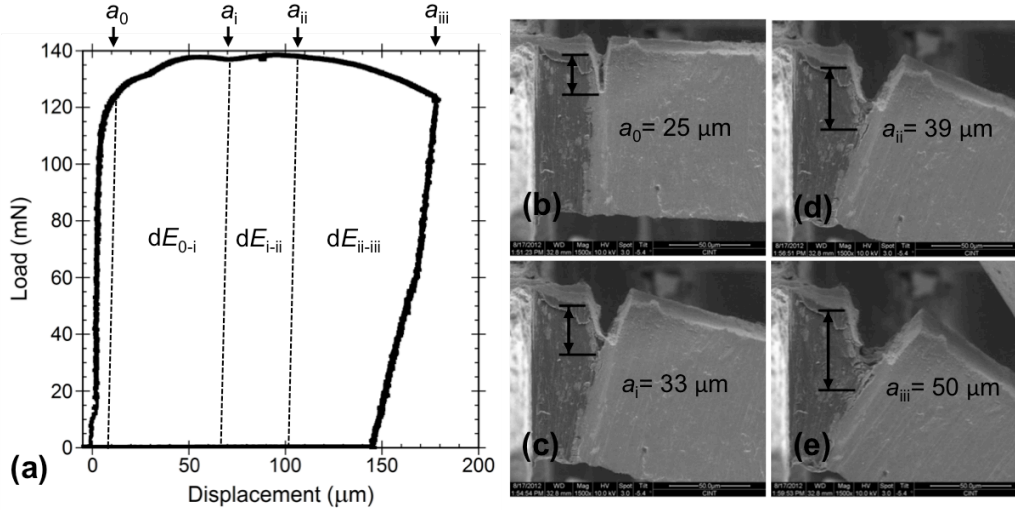


Figure 6: Al/Zr beam deflection showing (a) partitioning of energy, i.e., area under the load-displacement curve along with (b-e) four frames taken from the SEM in-situ movie with estimated crack lengths. The frames correspond to the locations indicated on the load-displacement curve. Calculations for the energy dissipation rate of this beam can be seen in Table 1.

Table 1: Energy dissipation rate for Al-Zr interface tested in the notched minicantilever geometry shown in Figure 6.

a (μm)	da (μm)	$2B*da$ (μm^2)	dE ($\mu\text{m}*m\text{N}$)	D (mJ/mm^2)
25				
33	8	1600	7952	5.0
39	6	1200	4416	3.7
50	11	2200	9591	4.4

The fracture energy dissipation rate for the Al/Zr interface ranged from 3.7-5 mJ/mm^2 . This is in close agreement with values obtained via bulge testing mentioned earlier in this article. During the portions of the load-displacement curve where crack growth occurs ($a = 25$ to $50 \mu\text{m}$), the energy dissipation rate only varies minimally, suggesting that despite the varying amounts of plastic deformation in the Al phase as the test progresses, the energy dissipation rate for the system remains the same. This further suggests that the amount of energy dissipated via plastic deformation of Al is very close to that required for crack propagation along the Al/Zr interface. An

EPFM analysis should become increasingly applicable in future work when materials and interfaces embrittled by the effects of radiation.

dU-10Mo/Zr interface:

For the dU-containing materials, two sets of beams were tested. One set had the Zr/dU-10Mo and Al/Zr interfaces buried within the substrate while the other had the both of the interface contained within the cantilever beam itself. In both cases, the beams were notched via FIB milling. For the buried interfaces, the FIB was also used to cut away excess material and expose only the Zr/dU-10Mo interface. As will be shown, interface location with respect to the base of the beam is very important. Fracture only occurs along and near the Zr/dU-10Mo interface when the interfaces are buried (then notched and excavated via FIB) beneath the base of the beam. When the interfaces are contained within the beam, fracture occurs along the Al/Zr interface even though the Zr/dU-10Mo interface is notched. In this case Al plastically deforms at a stress level that is inadequate to drive fracture along the Zr/dU-10Mo interface. A comparison showing the importance of interface location can be seen in Figure 7.

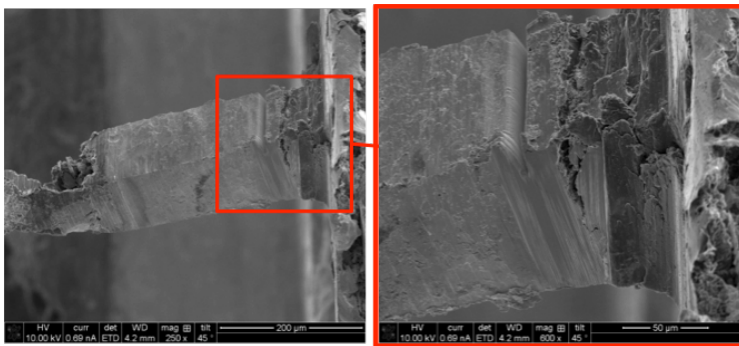


Figure 7: The notch for this beam was located at the Zr/dU-10Mo interface, however the crack propagated along the Al/Zr interface. This behavior was not seen for cantilever beams with both interfaces located under the base of the beam.

The dU beams with the buried Zr/dU-10Mo interface had a tapered geometry due to non-optimized milling. The larger cross-sectional area at the base required higher loads in order to plastically deform them enough to drive fracture. Therefore the hybrid testing technique (loading the cantilever beam using the Nanoindenter XP, pause after crack growth to image in the SEM) was used. As can be seen by comparing image (i) to image (ii) in Figure 8, the notch has initiated a crack that extends towards and along the Zr/dU-10Mo interface by approximately 12.9 μm . Since

the base of the beam is $185 \mu\text{m}$ wide, the new area generated is approximately $4790 \mu\text{m}^2$. In front of the crack-tip, there is an extended area of slip traces that could be considered a process zone. A lower bound estimate for new surface area is $4790 \mu\text{m}^2$. The energy expended during the bending is the area under the load-displacement curve and is $2.30 \times 10^7 \text{ mN}\cdot\text{nm}$. A portion of this energy was due to plastic deformation under the indenter tip that is represented by the load-displacement response of an indent into dU-10Mo in Figure 8 that is offset along the displacement axis by $20 \mu\text{m}$. The area corresponding to the indent is $0.23 \times 10^7 \text{ mN}\cdot\text{nm}$ giving the total energy expended at the base of the beam as $2.07 \times 10^7 \text{ mN}\cdot\text{nm}$. Therefore the strain energy dissipation rate is $D = 4.3 \text{ mJ}/\text{mm}^2$. Another example of Zr/dU-10Mo interfacial fracture is shown in Figure 9. In order to initiate a sharp crack from the notch, extra energy was necessary as is seen when calculating the energy from Figure 9, image (i) to image (ii). Once the sharp crack was initiated, energies decreased to $5.9 \text{ mJ}/\text{mm}^2$. On average the energy dissipation rate of the Zr/dU-10Mo interface was $4\text{-}6 \text{ mJ}/\text{mm}^2$.

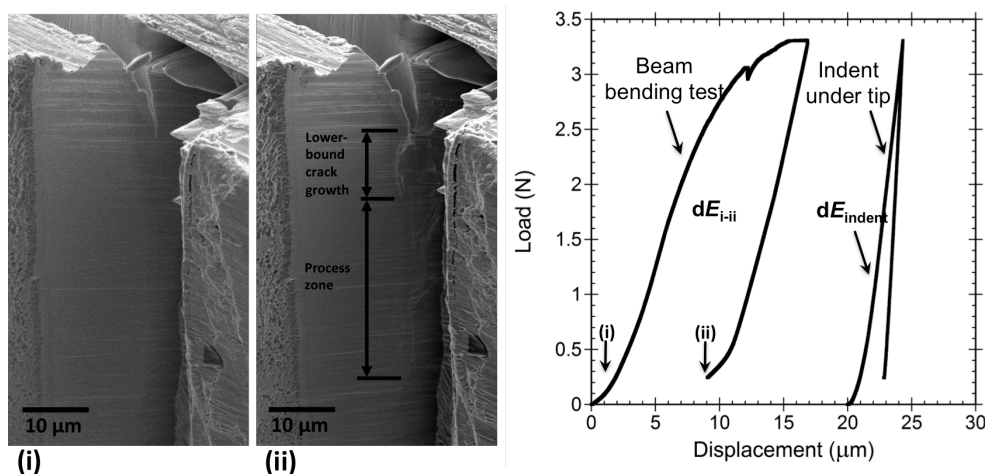


Figure 8: Fracture along the Zr/dU-10Mo interface where image (i) is the initial notch before the test, the location of which is shown on the load-displacement curve, and image (ii) is after the first compression as shown on the load-displacement curve. Since the maximum load here was greater than 3 N, plastic deformation was generated beneath the tip and is represented by area under the curve. In order to account for this deformation, the area generated from the indent is subtracted from the overall energy of the test.

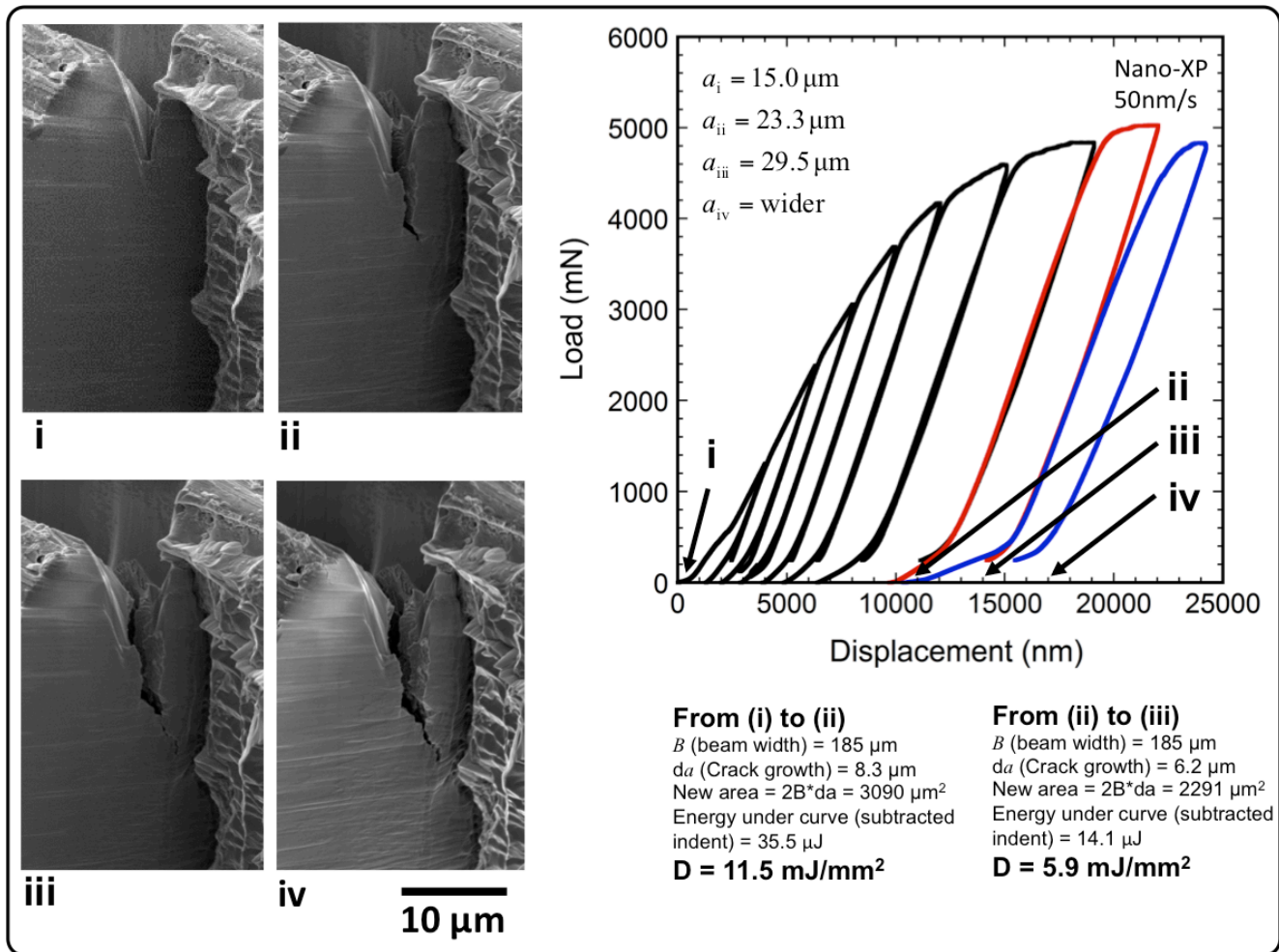


Figure 9: Zr/dU-10Mo interfacial fracture where strain energy dissipation rates were initially high. Once a sharp crack was nucleated as seen in image (ii), the dissipation rates decreased to approximately 5.9 mJ/mm².

Concluding Remarks:

In this work, the fracture behavior of Al/Zr and Zr/dU-10Mo interfaces was measured via the minicantilever bend technique. The energy dissipation rates were found to be approximately 3.7-5 mJ/mm² and 4.0-5.9 mJ/mm² respectively. The values for the Al/Zr fracture energy release rates were in good agreement with those found through miniaturized disc bulge testing, while the values for the minicantilever-tested Zr/dU-10Mo interface were higher by nearly an order of magnitude with respect to values obtained using the miniaturized disc bulge test. This discrepancy can be attributed to the area of interfacial content measured by each test technique. That is, the miniaturized disc bulge test encompasses a larger amount of interfacial content, and so any inhomogeneity or weakness in the Zr/dU-10Mo interface is more statistically likely to limit

fracture toughness in this test method. However, the minicantilever test measures local fracture behavior at reduced interfacial areas. As such, the miniaturized bulge test represents a lower bound fracture toughness associated with inhomogeneities at the interface, whereas the minicantilever test represents an upper-bound fracture toughness value of a “pristine” interface. More minicantilever tests would have to be carried out in order to begin to see the effects of inhomogeneities as was witnessed in the miniaturized bulge test. It was found that in order to test the Zr/U-10Mo interface, location of the hinge of the cantilever was a key parameter. While this test could be adapted to hot cell use through careful alignment fixturing and measurement of crack lengths with an optical microscope (as opposed to SEM, which was used here out of convenience), machining of the cantilevers via MiniMill in such a way as to locate the interfaces at the cantilever hinge, as well as proper placement of a femtosecond laser notch will continue to be key challenges in a hot cell environment. Additionally, the expected interfacial embrittlement after irradiation may limit the amount of ductility found in the aluminum phase, and if so, linear elastic fracture mechanics may prove sufficient for further calculation of the fracture toughness of the interfaces in Al/Zr/U-10Mo fuel elements.

Acknowledgements:

The authors would like to acknowledge the financial support of the US Department of Energy Global Threat Reduction Initiative Reactor Convert program. This work was performed, in part, at the Center for Integrated Nanotechnologies, an Office of Science User Facility operated for the U.S. Department of Energy, Office of Science. Los Alamos National Laboratory, an affirmative action equal opportunity employer, is operated by Los Alamos National Security, LLC, for the National Nuclear Security Administration of the U.S. Department of Energy under contract DE-AC52-06NA25396.

References:

1. H. Ozaltun and P.G. Medvedev, *Structural behaviour of monolithic fuel plates during hot isostatic pressing and annealing*, in *RRFM 2010: 14. international topical meeting on Research Reactor Fuel Management (RRFM), Marrakech (Morocco), 21-25 Mar 2010*; . p. 11.
2. A.B. Robinson, G.S. Chang, D.D. Keiser, D.M. Wachs, and D.L. Porter, *Irradiation performance of U-Mo alloy based "monolithic" plate-type fuel*, 2009, Idaho National Laboratory.

3. J.M. Wight, G.A. Moore, and S.C. Taylor, *TESTING AND ACCEPTANCE OF FUEL PLATES FOR RERTR FUEL DEVELOPMENT EXPERIMENTS*, in *RERTR 2008 International Meeting on Reduced Enrichment for Research and Test Reactors*, Hamilton Crowne Plaza Hotel in Washington D.C., 10/05/2008, 10/09/2008: 2008: United States.
4. D.D. Keiser, J.F. Jue, and D.E. Burkes, *Characterization and testing of monolithic RERTR fuel plates*, in *11th International topical meeting. Research Reactor Fuel Management (RRFM) and meeting of the International Group on Reactor Research (IGORR)*, Lyon (France), 11-15 Mar 2007; 2007: France. p. 111.
5. D.E. Burkes, D.D. Keiser, D.M. Wachs, J.S. Larson, and M.D. Chapple, *Characterization of monolithic fuel foil properties and bond strength*, in *11th International topical meeting. Research Reactor Fuel Management (RRFM) and meeting of the International Group on Reactor Research (IGORR)*, Lyon (France), 11-15 Mar 2007; 2007: France. p. 426.
6. G.A. Moore, B.H. Rabin, J.F. Jue, C.R. Clark, N.E. Woolstenhulme, B.H. Park, et al. *Development Status of U10Mo Monolithic Fuel Foil Fabrication at the Idaho National Laboratory*. in *RERTR 2010*. 2010. Lisbon, Portugal.
7. J. Katz, K. Clarke, B. Mihaila, J. Crapps, B. Aikin, V. Vargas, et al. *Scale-up of the HIP bonding process for aluminum clad LEU reactor fuel*. in *RERTR 2011*. 2011. Santiago, Chile.
8. J.-F. Jue, B.H. Park, C.R. Clark, G.A. Moore, and D.D. Keiser Jr, *Nuclear Technology*, 172, 204).
9. N.A. Mara, J. Crapps, T. Wynn, K. Clarke, P. Dickerson, D.E. Dombrowski, et al. *Nanomechanical Behavior of U-10Mo/Zr/Al Fuel Assemblies*. in *RERTR 2011*. 2011. Santiago, Chile.
10. N.A. Mara, J. Crapps, T. Wynn, K. Clarke, A. Antoniou, P. Dickerson, et al., Submitted to: *Philosophical Magazine*, (2012).
11. J.D.G. Sumpter. *Fracture toughness - a measurable materials parameter*. in *FRACTURE, PLASTIC FLOW AND STRUCTURAL INTEGRITY*. 1 CARLTON HOUSE TERRACE, LONDON SW1Y 5DB, ENGLAND: IOM COMMUNICATIONS LTD.